Electronic Supplementary Information for:

Edge-carboxylated graphene nanosheets *via* ball milling

In-Yup Jeon,[†] Yeon-Ran Shin,[†] Gyung-Joo Sohn,[†] Hyun-Jung Choi,[†] Seo-Yoon Bae,[†] Javeed Mahmood,[†] Sun-Min Jung,[†] Jeong-Min Seo,[†] Min-Jung Kim,[†] Dong Wook Chang,[†] Liming Dai[†,‡]* and Jong-Beom Baek[†,]*

[†] Interdisciplinary School of Green Energy/Institute of Advanced Materials & Devices, Ulsan National Institute of Science and Technology (UNIST), 100 Banyeon, Ulsan 689-798, South Korea

[‡] Department of Macromolecular Science and Engineering, Case Western Reserve University, 10900 Euclid Avenue, Cleveland, Ohio 44106, USA.

*To whom correspondence should be addressed. E-mail: jbbaek@unist.ac.kr (J.-B. Baek); liming.dai@case.edu (L. Dai)

Experimental

Instrumentations. Fourier transform infrared (FTIR) spectra were recorded on Perkin-Elmer Spectrum 100 using KBr disks. Differential scanning calorimety (DSC) while themogravimetric analysis (TGA) were conducted on a TA Q200 (TA Instrument) under nitrogen at a heating rate of 10 °C/min. The surface area was measured by nitrogen adsorption-desorption isotherms using the Brunauer-Emmett-Teller (BET) method on Micromeritics ASAP 2504N. The field emission scanning electron microscopy (FE-SEM) was performed on FEI Nanonova 230 while the high-resolution transmission electron microscopy (HR-TEM) employed in this work is a JEOL JEM-2100F (Cs) microscope operating at 200 kV. The TEM specimen were prepared by dipping carbon micro-grids (Ted Pella Inc., 200 Mesh Copper Grid) into well-dispersed samples in NMP or ethanol. X-ray photoelectron spectra (XPS) were recorded on a Thermo Fisher K-alpha XPS spectrometer. Elemental analysis (EA) was conducted with Thermo Scientific Flash 2000. Zeta-potential values were determined using a Malvern Zetasizer (Nano ZS, Malvern Instruments). X-Ray diffraction (XRD) patterns were recorded with a Rigaku D/MAZX 2500V/PC with Cu–Kα radiation (35 kV, 20 mA, λ = 1.5418 Å). Raman spectra were taken with a He-Ne laser (532 nm) as the excitation source by using confocal Raman microscopy (Alpha 300S, WITec, Germany), in conjunction with atomic force microscopy (AFM). Solid state ^{13}C magic angle spinning (MAS) NMR spectrum was recorded on a Varian Unitylnova 600 (600 MHz) spectrometer, using a 5-mm probe spinning at 9 kHz. The resistance/conductivity of film samples was measured by four point probe method using Advanced Instrument Technology (AIT) CMT-SR1000N.

General procedure for edge-carboxylation of graphite (ECG) by ball milling. In a typical experiment, the ball milling of graphite was carried out in a planetary ball-mill machine

(Pulverisette 6, Fritsch; Fig. S1a) in the presence of dry ice at 500 rpm. To start with, 5 g of the pristine graphite (Alfa Aesar, natural graphite, 100 mesh (< 150 μm), 99.9995% metals basis, Lot#14735, Fig. S1b) and 100 g of dry ice (Hanyu Chemical Inc.) for ECG, NH_3 (1.52 g) for EAG or SO_3 (7.0 g) for ESG were placed into a stainless steel capsule containing stainless steel balls of 5 mm in diameter (Fig. S1b). The container was then sealed and fixed in the planetary ball-mill machine (Fig. S1c), and agitated with 500 rpm for 48h. Thereafter, the built-up internal pressure was maintained *ca.* 5 bar and very slowly released through a gas outlet (Fig. S1c). Upon opening the container lid in air at the end of ball milling, sparkling occurred (Figs. S1d and S1e, and Supplementary video) due to the hydration of carboxylates into carboxylic acids by the air moisture, as schematically shown in Fig. 1d. The resultant product was further Soxhlet extracted with 1M aqueous HCl solution to completely acidify carboxylates and to remove metallic impurities, if any. Final product was freeze-dried at -120 °C under a reduced pressure (0.05 mmHg) for 48h to yield 6.28 g of ECG as dark black powder (Fig. 1c). Found: C, 72.04%; H, 1.01%; O, 26.46%. 5.25 g of EAG as dark black powder. Found: C, 88.83%; H, 1.21%; N, 4.49%; O, 3.69%. 5.03 g of ESG as dark black powder. Found: C, 79.58%; H, 0.62%; O, 9.36%; S, 9.35%.

Synthesis of graphite oxide by modified Hummers' process. Pristine graphite (3.0 g) was mixed with 1.5 g of $NaNO_3$ and 75 mL of concentrated H_2SO_4. The mixture was cooled down to 0 °C in an ice bath and stirred for 2h. Then, 9.0 g of $KMNO_4$ was added slowly (temperature was maintained at <5 °C throughout the mixing), and continuously stirred for another hour. The cooling bath was then removed and the mixture was cooled down to room temperature. To this, ~100 mL of distilled water was added (gas evolved) and the temperature was increased to 90 °C in an oil bath. After reaching 90 °C, 300 mL of water was added again and continuously stirred for another hour and a half. The color of the mixture turned to mud

brown. This mixture was then treated with 30 mL of 30% H_2O_2 and ~3 liters of hot water was added and diluted. The mixture was further washed with excess water until the pH of the filtrate was nearly neutral, finally vacuum filtered and freeze-dried under reduced pressure (0.5 mmHg) at -120 °C for 48 h to yield GO.

Preparation of ECG and GO thick films by compression molding. ECG and GO samples were compressed 3000 bar by hydraulic press (Specac Inc, Model No.: 21984) to produce ECG and GO thick films (Fig. 4b (i&ii)), respectively.

Preparation of the H-ECG/PET thin films by solution casting. Large-area graphene films were made with different ECG concentrations in NMP. These solutions were cast on a SiO_2(300 nm)/Si wafer and subsequently heat-treated at 900 °C in argon for 2h. To transfer the solution-cast H-ECG films onto other substrates, poly(methylmethaacrylate) (PMMA) solution in tetrahydrofuran (THF) was spin coated on the H-ECG films. The SiO_2 substrate was then etched off by floating on an aqueous solution of 1M hydrofluoric acid (HF). Thereafter, the H-ECG on PMMA (H-ECG/PMMA) films were transferred to poly(ethylene terephthalate) (PET) films and the PMMA was washed off by immersing in acetone to produce H-ECG on PET (H-ECG/PET) (Fig. 4c). Six different H-ECG/PET thin films with approximately 3.5 × 5 cm dimensions were tested, though many larger H-ECG films on various substrates can be readily prepared through the similar procedure. The optical transmittances and sheet resistances of the films were measured by using UV-vis spectroscopy and four-point probe, respectively, and were found to be in the range of 4.6-86.0% (Fig. 4d) and 0.58-53.0 kΩ/sq (Fig. 4e). The thickness was estimated on the basis of 2.3% light absorption per graphitic layer at 550 nm, which has thickness of 0.34 nm (S1).

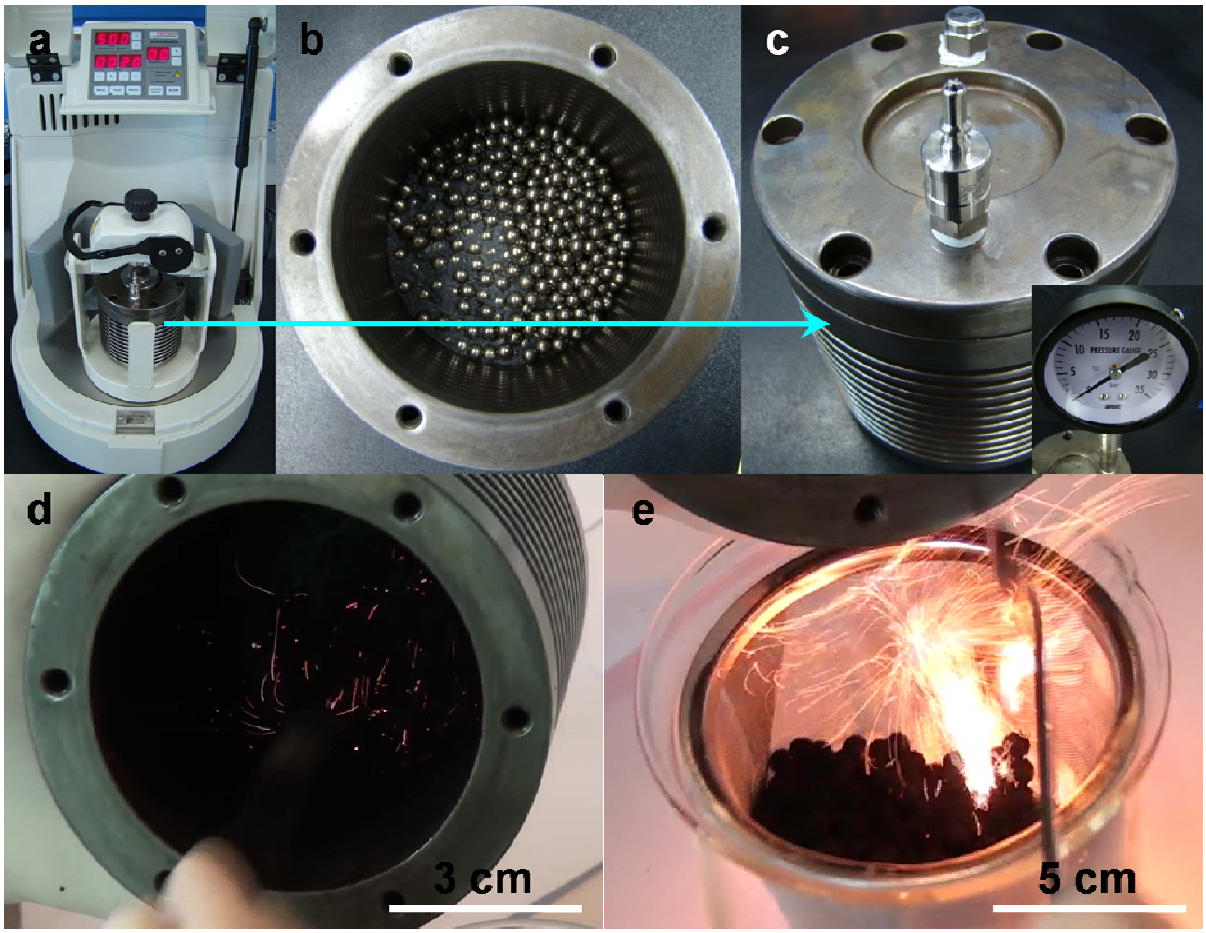

Fig. S1. (a) Ball milling apparatus; **(b)** ball mill capsule with graphite and stainless balls (diameter = 5 mm); **(c)** ball mill capsule assembled with gas inlet and outlet. Inset is pressure gauge; **(d)** After 48h ball milling, ECG was sparkling in a ball mill container upon opening the lid; **(e)** violent sparkling occurred when ECG was exposure to ambient air. The images were captured from the Supplementary video clip.

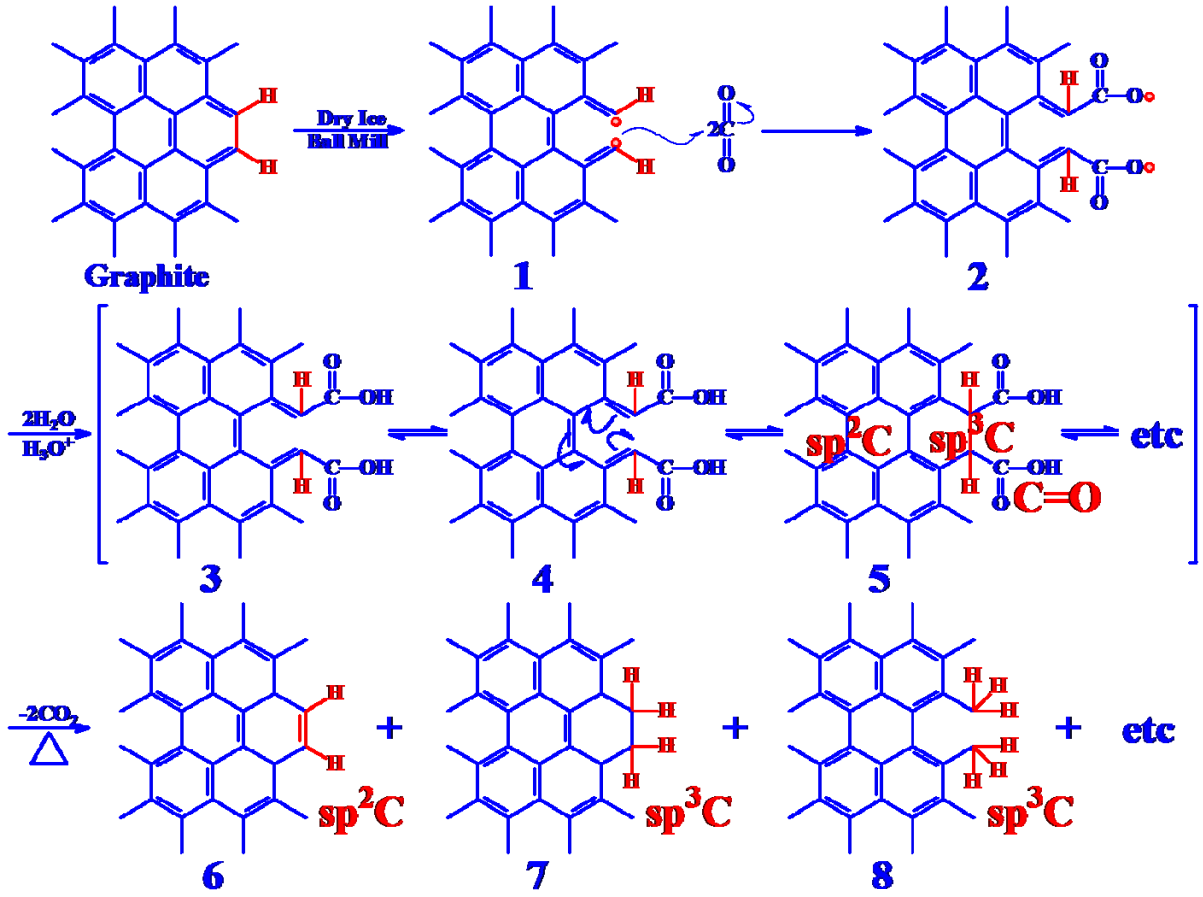

Fig. S2. Proposed mechanism for the edge-carboxylation and thermo-decarboxylation. The graphitic structure is simplified for the reason of clarity.

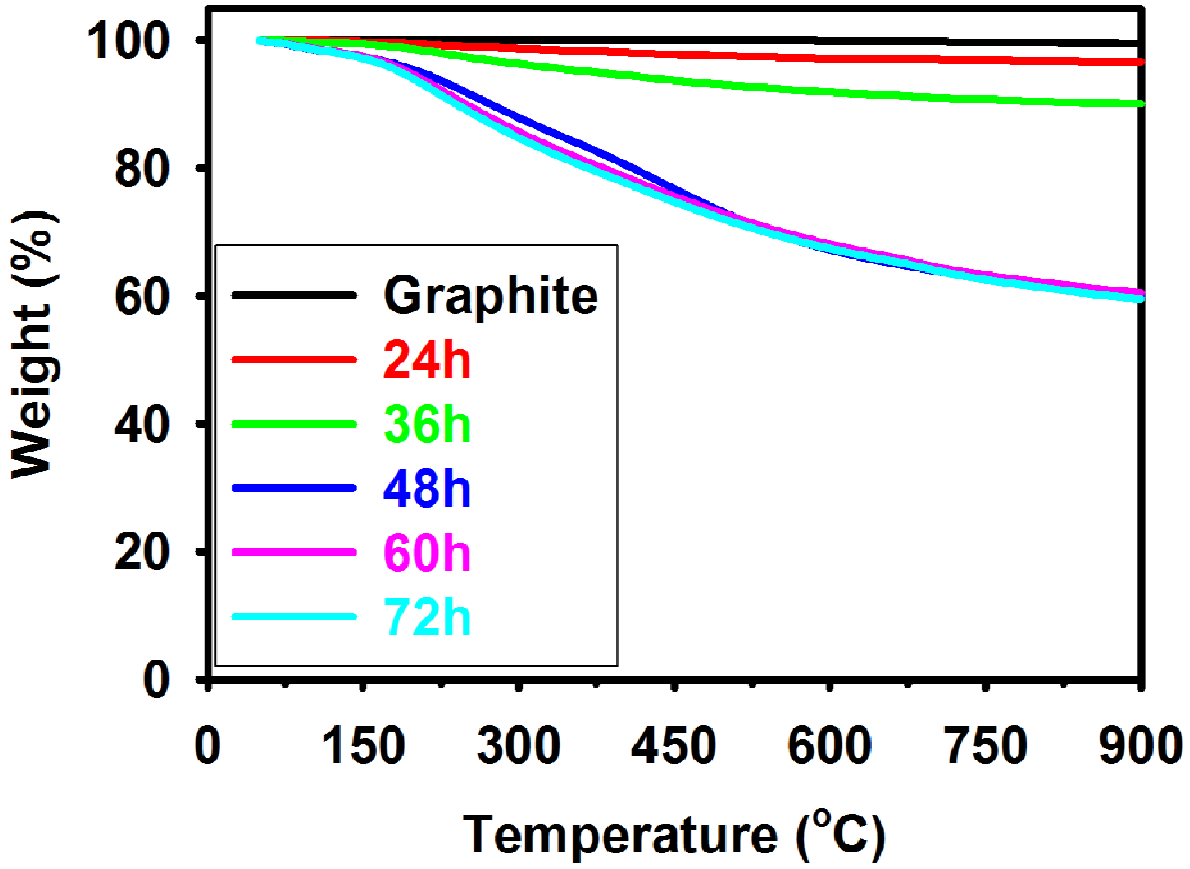

Fig. S3. TGA thermograms for ECG samples prepared with different ball milling times. The heating rate was 10 °C/min in nitrogen. The degree of carboxylation remained almost constant after 48h ball milling, implying a steady state was reached at 48h.

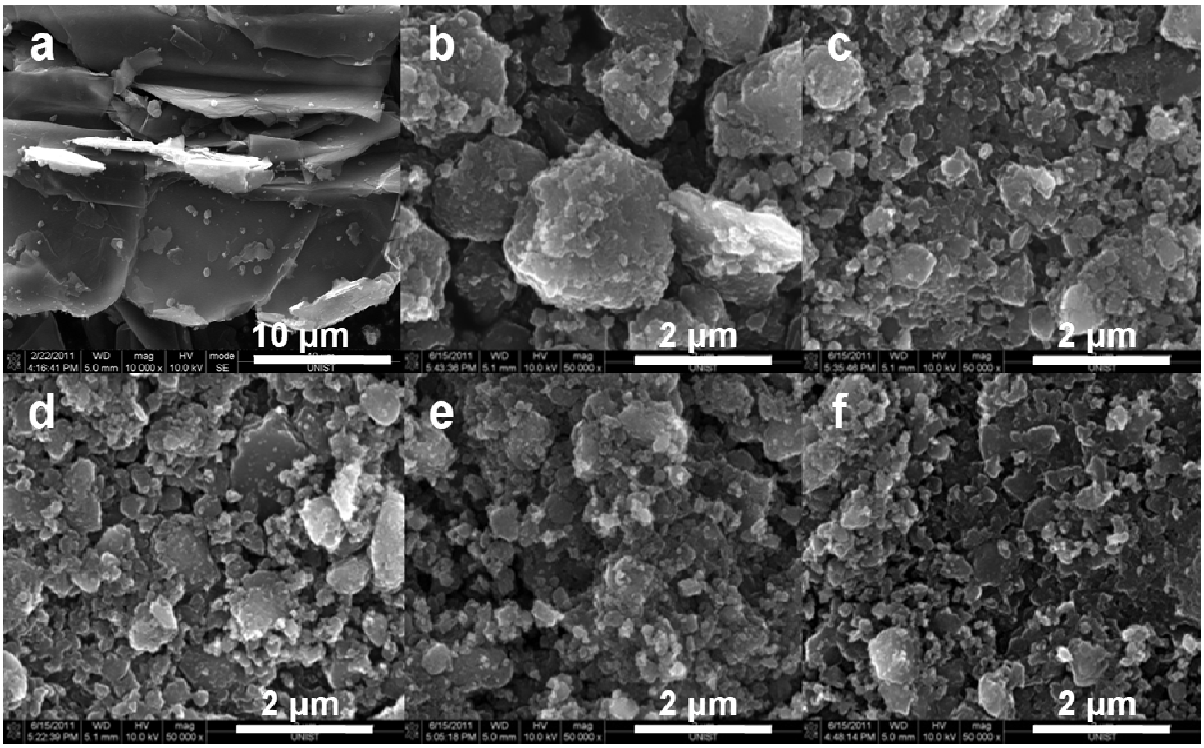

Fig. S4. SEM images: **(a)** the pristine graphite. **(b)** ECG-24 h, **(c)** ECG-36 h, **(d)** ECG-48 h, **(e)** ECG-60 h, and **(f)** ECG-72 h. The grain size of graphitic platelets drastically decreased with the balling time until 48h.

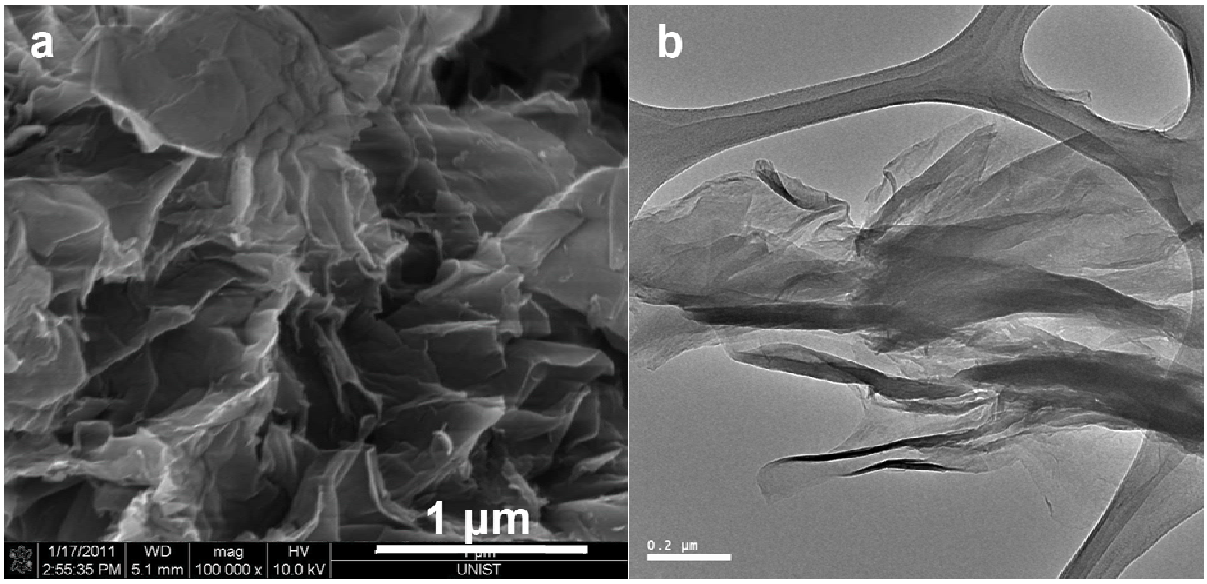

Fig. S5. (a) SEM and **(b)** TEM images of GO prepared by the modified Hummers' process.

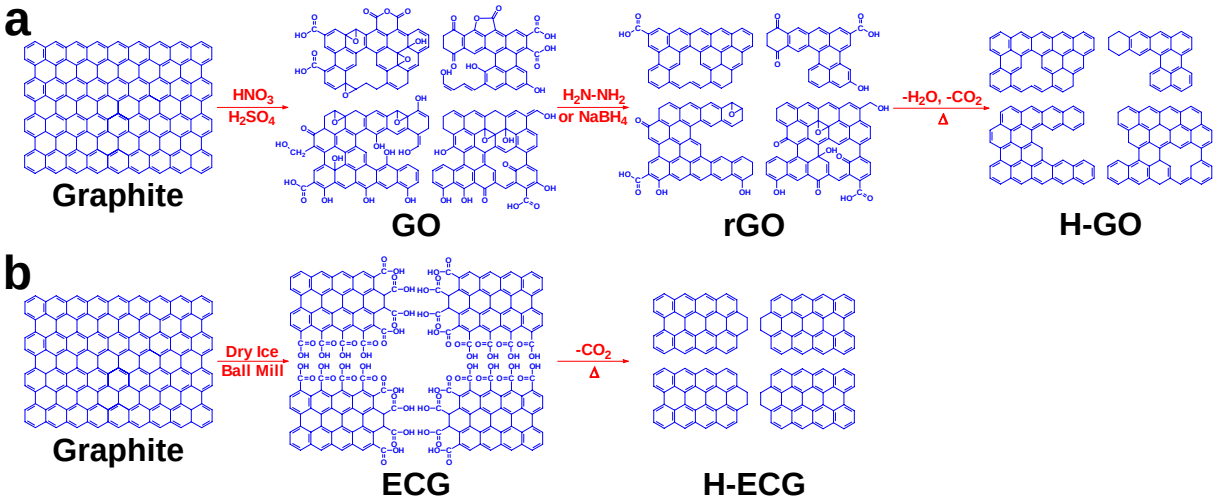

Fig. S6. (a) Syntheses and proposed structures of graphene oxide (GO), reduced graphene oxide (rGO) and heat treated GO (H-GO) reported by Lerf, *et al.* (S2) and Gao, *et al*. (S3). **(b)** Syntheses and proposed structures of edge-carboxylated graphene (ECG) and heat-treated (decarboxylated) ECG (H-ECG).

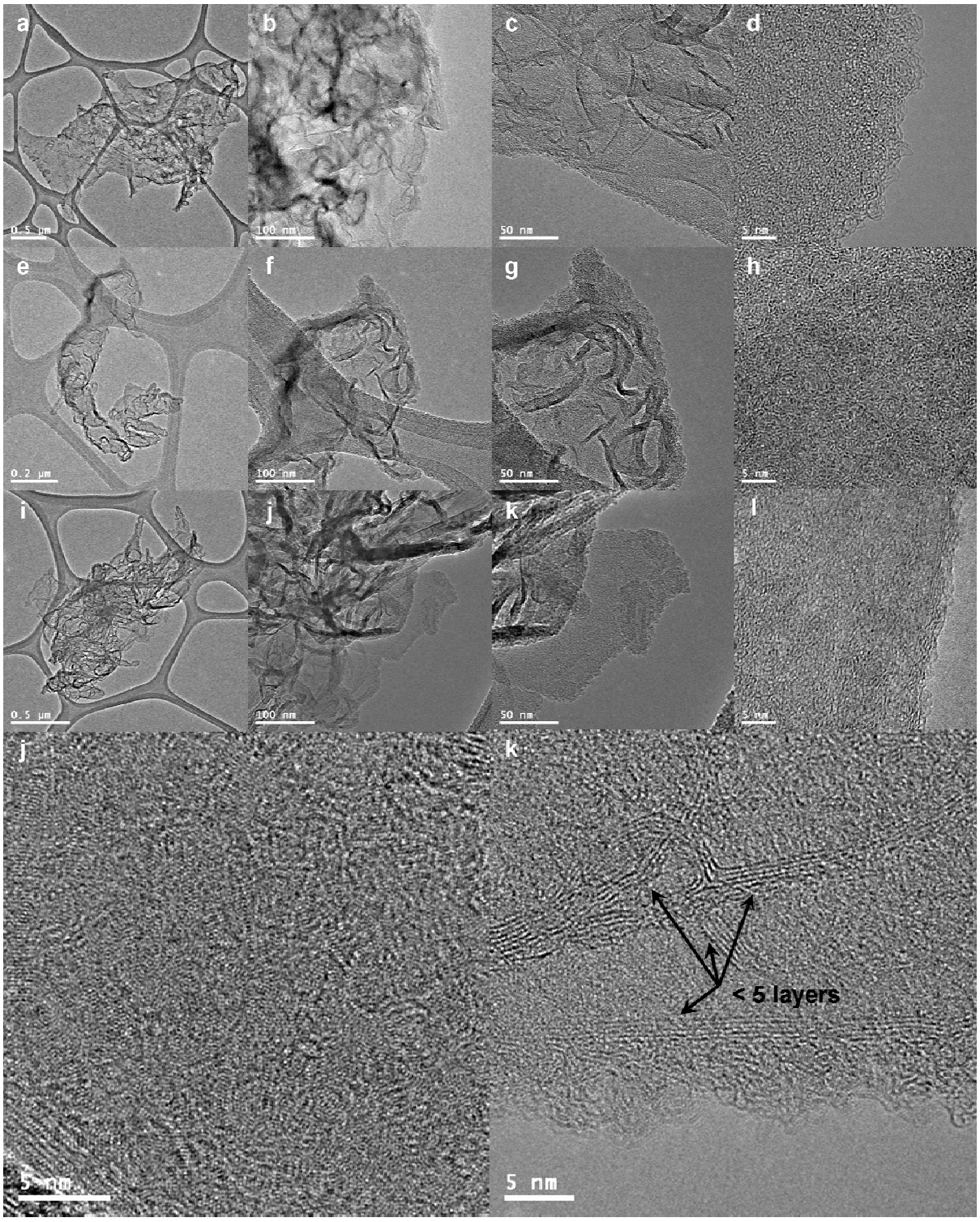

Fig. S7. TEM images for various randomly selected ECGs at different magnifications: Sample 1 **(a) to (d)**, Sample 2: **(e) to (h)**, Sample 3 **(i) to (l)**, and Sample 4 **(j) to (k)**. Maximum number of layers is approximately 5.

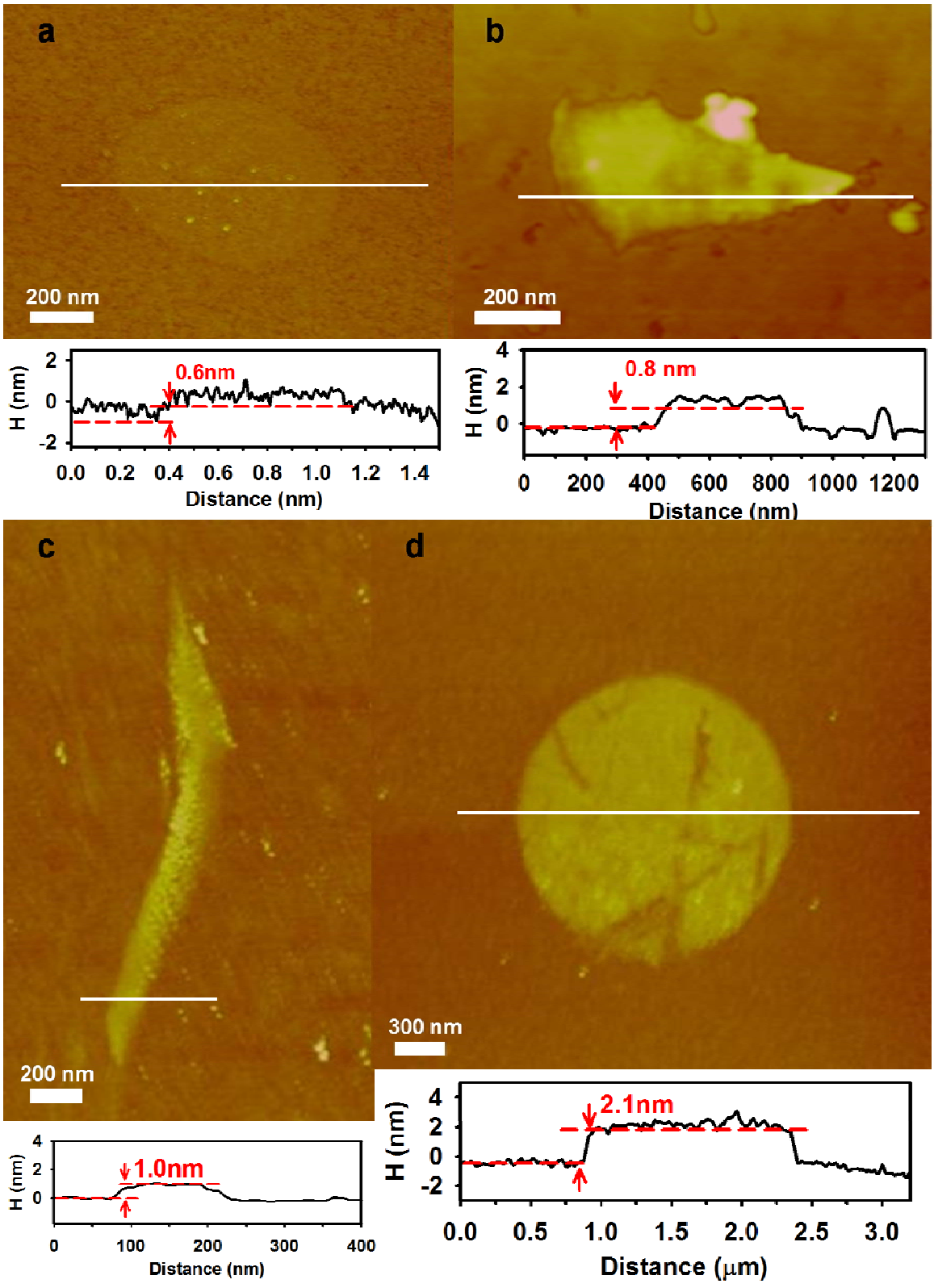

Fig. S8. AFM images with topographic height profiles: **(a** and **b)** single layer; **(c** and **d)** a few layers.

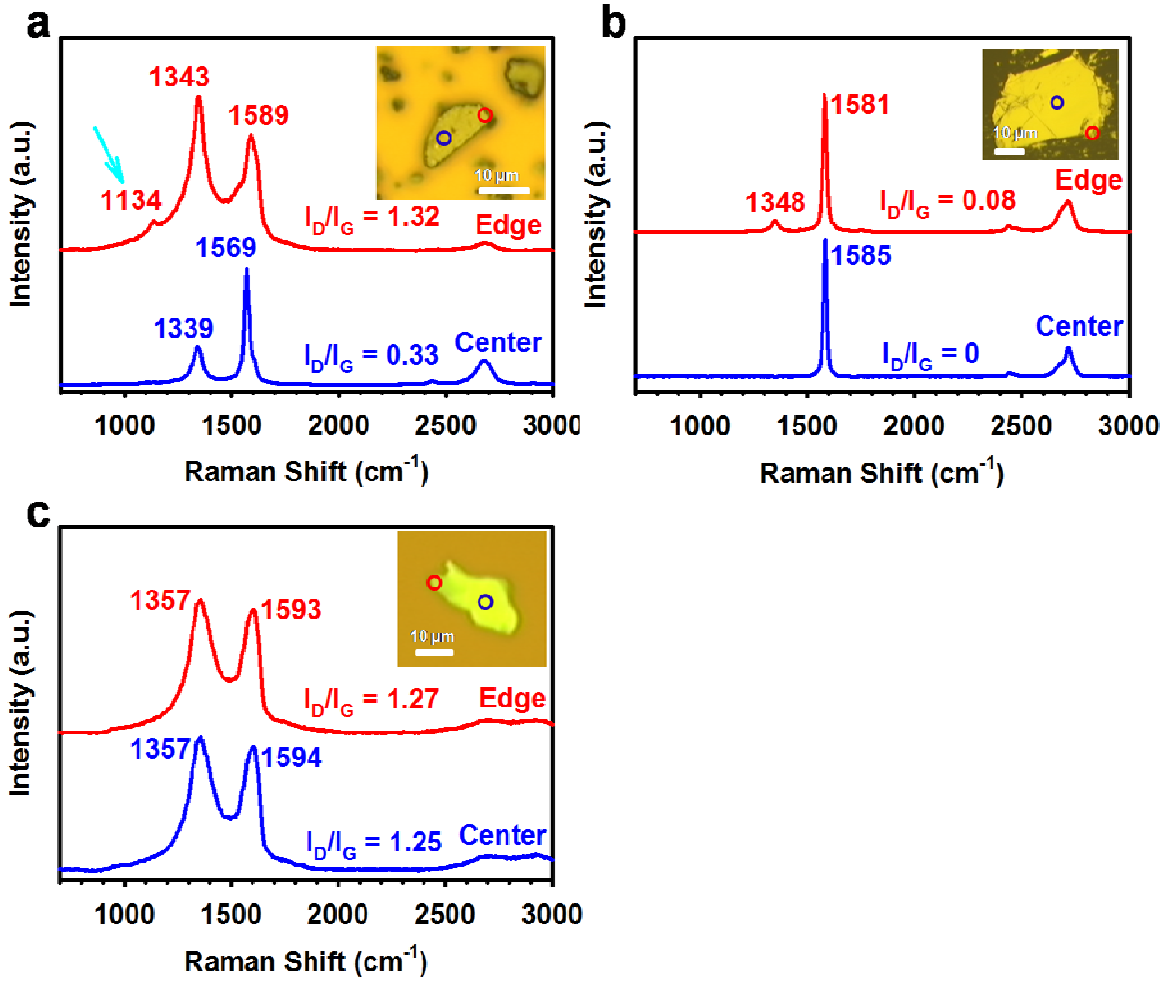

Fig. S9. Micro-Raman spectra recorded at the edge and on the basal plane: **(a)** a relatively large ECG flake after being ball-milled for 24 h; **(b)** pristine graphite flake; **(c)** GO flake. Insets are confocal optical microscopy image of D and G bands.

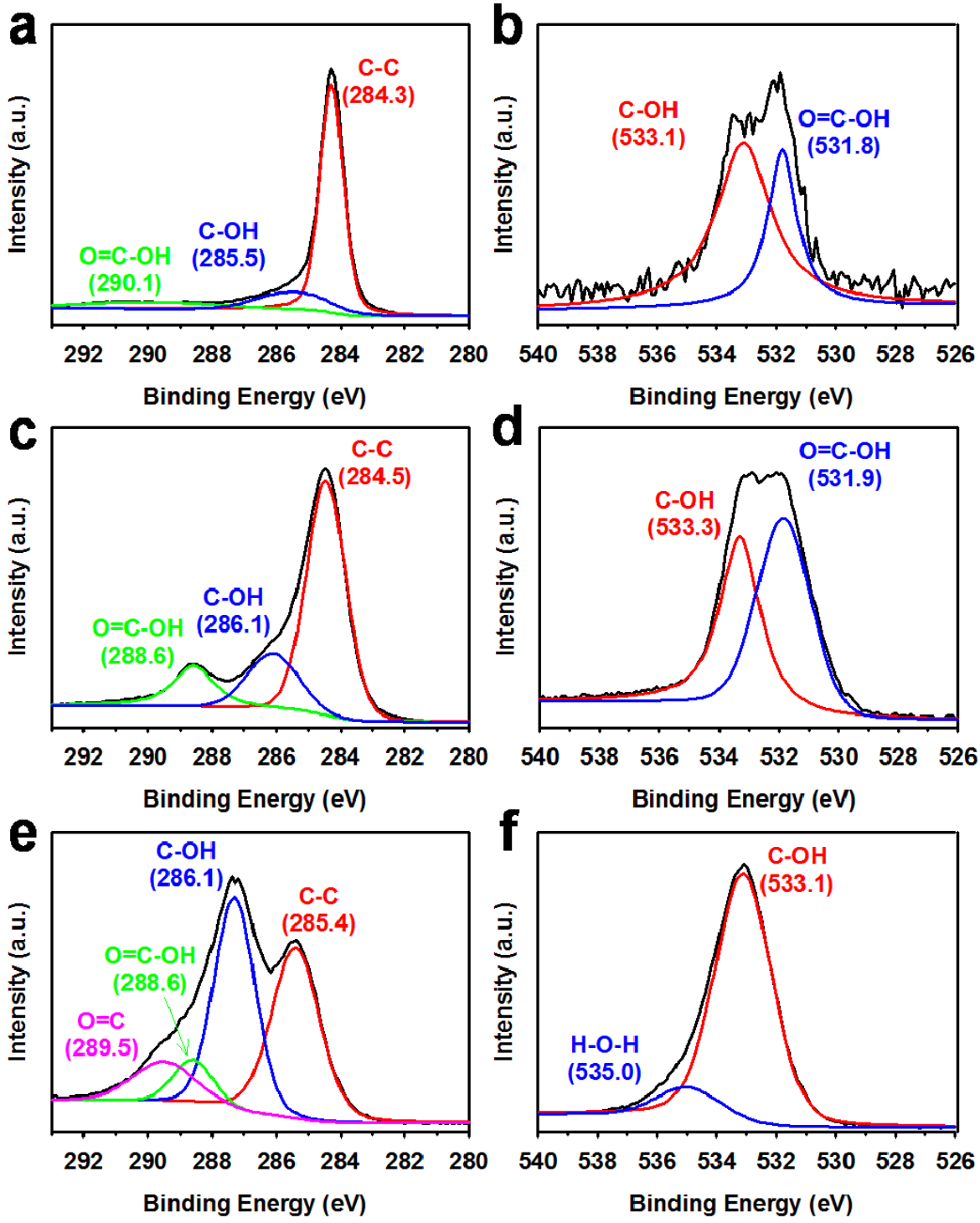

Fig. S10. High resolution XPS spectra: **(a)** C 1s and **(b)** O 1s of the pristine graphite; **(c)** C 1s and **(d)** O 1s of ECG; **(e)** C 1s and **(f)** O 1s of GO.

XPS is a powerful tool to compare relative amount of elements in bulk state. However, element contents from XPS analyses could not be absolute values like EA, because XPS is more sensitive to surface chemical composition (S4). As seen in Fig. S10a, the pristine graphite shows a typical C 1s peak at 284.3 eV associated with the graphitic C-C, along with two very weak sub-bands assignable to *C*-*O*H and O=*C*-*O*H at 285.5 and 290.1 eV, respectively. The pristine graphite also shows a minor O 1s peak at 532.1 eV (Fig. 3d and S10b), which is mostly related to physically adsorbed oxygen/moisture for *C*-*O*H (S5). In the case of ECG, the C 1s peak consists of graphitic C-C centered at 284.5 eV with much higher peak intensities for *C*-*O*H (286.1 eV) and O=*C*-*O*H (288.6 eV) (Fig. S10c) than those for the pristine graphite (Fig. S10a) (S6-S8). The O 1s spectrum of ECG also showed *C*-*O*H and O=*C*-*O*H peaks at 531.9 and 533.3 eV, respectively (Fig. S10d). The edge groups of ECG are mostly carboxylic acids with high oxygen content of 17.18 %. Since ECG is edge-selectively carboxylated, C 1s and O 1s peak are very different from those of GO (Fig. S10e and S10f) (S9,S10). GO has many different oxygenated groups, such as hydroxyl, epoxy, carboxyl and others (S2). GO has the graphitic C-C at 285.4 eV as a second major peak, while *C*-*O*H at 286.1 eV is a major peak that is attributable to both *C*-*O*H and O=*C*-*O*H. Together with FTIR (see, Fig. 3a), mixed C-O responses from *C*-*O*H and O=*C*-*O*H in GO are completely distinguishable. More clearly, GO has a single major O 1s peak at 533.1 eV for *C*-*O*H and O=C-OH at 531.9 eV except very minor peak at 535 eV for physically absorbed moisture as observed in TGA (see, Fig. S14b) and DSC (Fig. S14c) (S11).

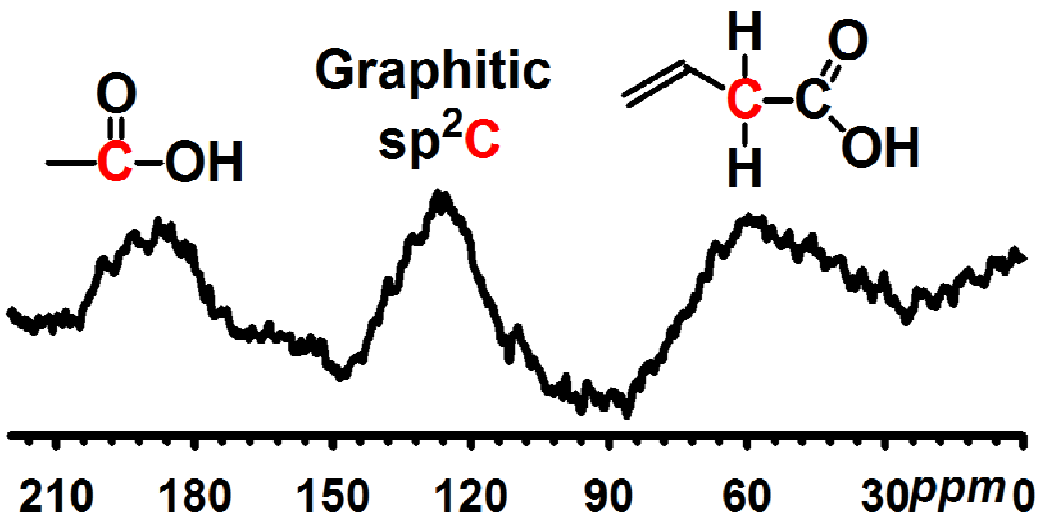

Fig. S11. Solid-state ^{13}C magic-angle spinning (MAS) NMR spectra of ECG. A direct ^{13}C pulse spectrum obtained with 12 kHz MAS and a 90° ^{13}C pulse (40,000 scans). The peak at around 60 ppm is caused by the carbons where carboxylic acid attached sp^3C (highlighted in red, structure 5 in Fig. 3). The peaks at around 130 and 190 ppm are graphitic sp^2C and carbonyl (C=O) in carboxylic acid, respectively.

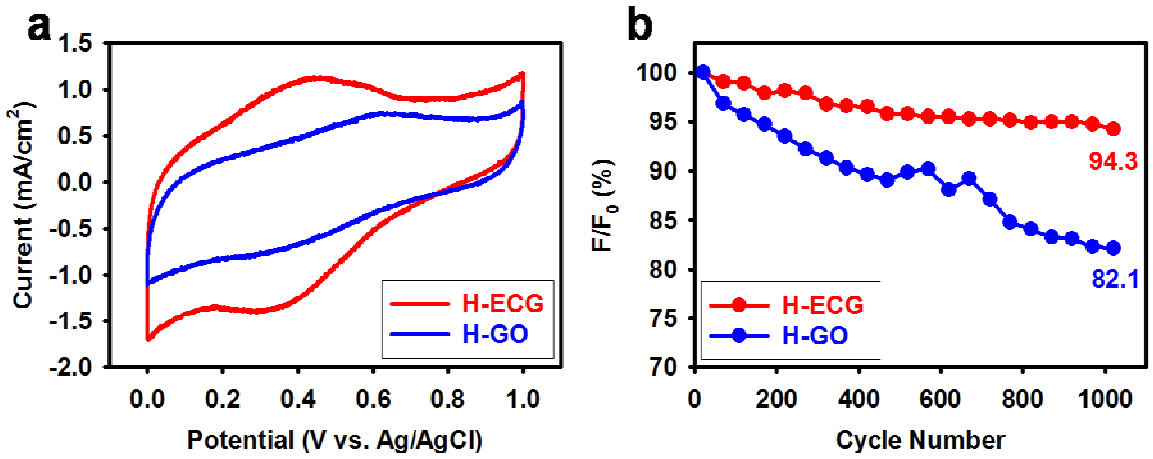

Fig. S12. (a) Cyclic voltammograms of samples/glassy carbon (GC) electrodes in 0.1 M aq. H_2SO_4 solution with a scan rate of 0.1 V/s; **(b)** relative capacitance changes with respect to cycle number at 0.1 V/s. H-ECG and H-GO maintain 94.3 and 82.1 % of initial capacitance, respectively.

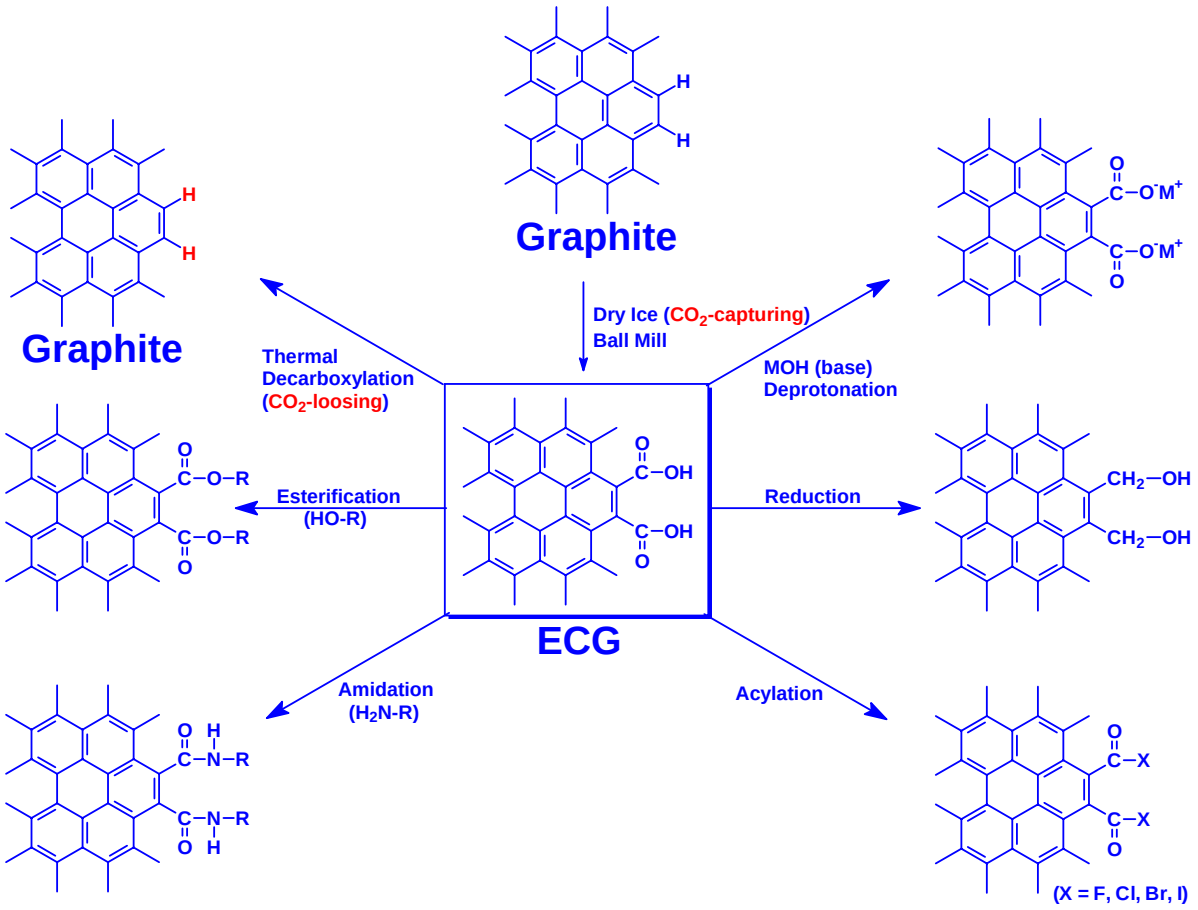

Fig. S13. Various derivatization reactions from aromatic carboxylic acids.

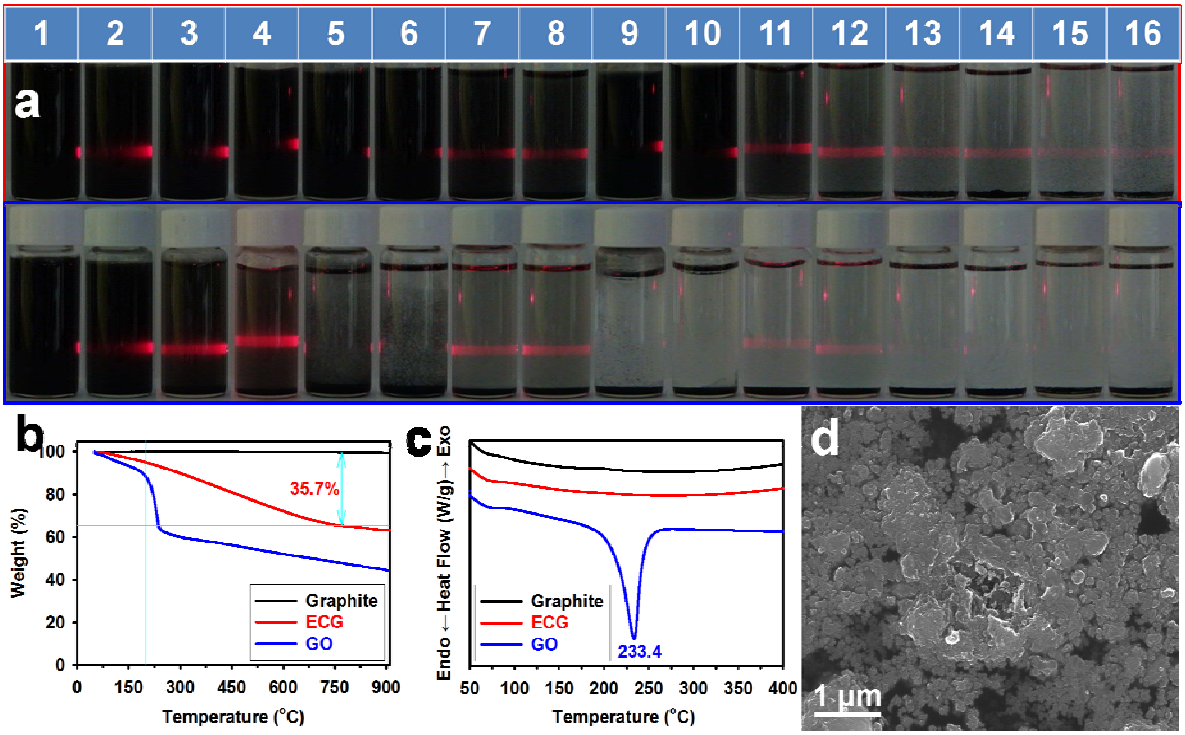

Fig. S14. (a) Solubility of ECG in various solvents: (1) NMP; (2) IPA; (3) 7M NH_4OH; (4) H_2O; (5) hexane; (6) toluene; (7) DMF; (8) DMAc; (9) 1M HCl; (10) 1M KOH; (11) 1M NH_4OH; (12) MeOH; (13) THF; (14) ethyl acetate; (15) acetone; (16) CH_2Cl_2: (top) after 30s; (bottom) after 1 week. **(b)** TGA thermograms of graphite, ECG and GO with a ramping rate of 10 °C/min in nitrogen; **(c)** DSC thermograms of graphite, ECG and GO with a ramping rate of 10 °C/min in nitrogen; **(d)** SEM image of ECG after dispersed in NMP and reaggregated.

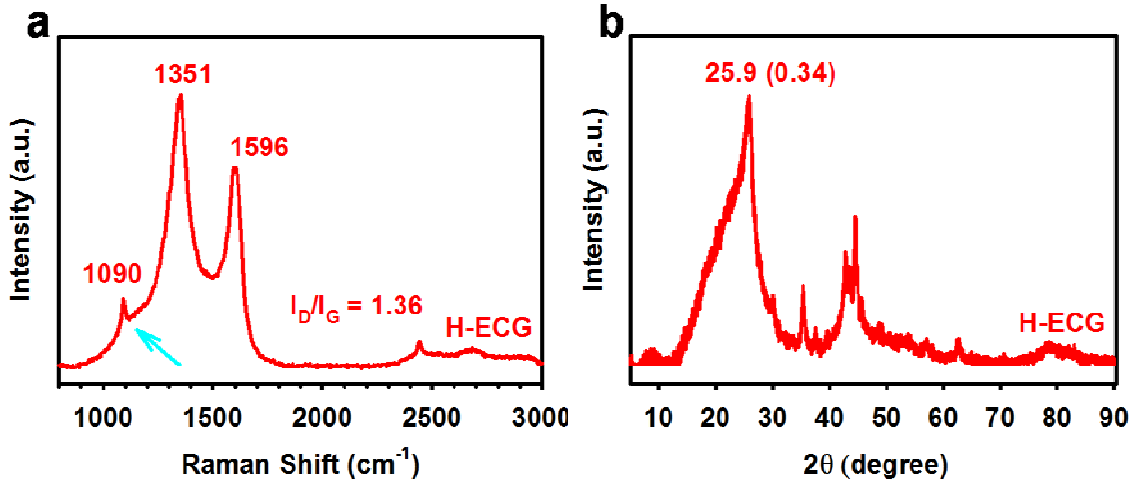

Fig. S15. Heat-treated ECG (H-ECG) at 900 °C for 2 h: **(a)** Raman spectra, showing a peak at 1090 cm^{-1} attributable to sp^3C-H as highlighted in **7** and **8** in Fig. S2 (S12); **(b)** XRD diffraction pattern, showing strong peak at 25.9° (d-spacing = 0.34).

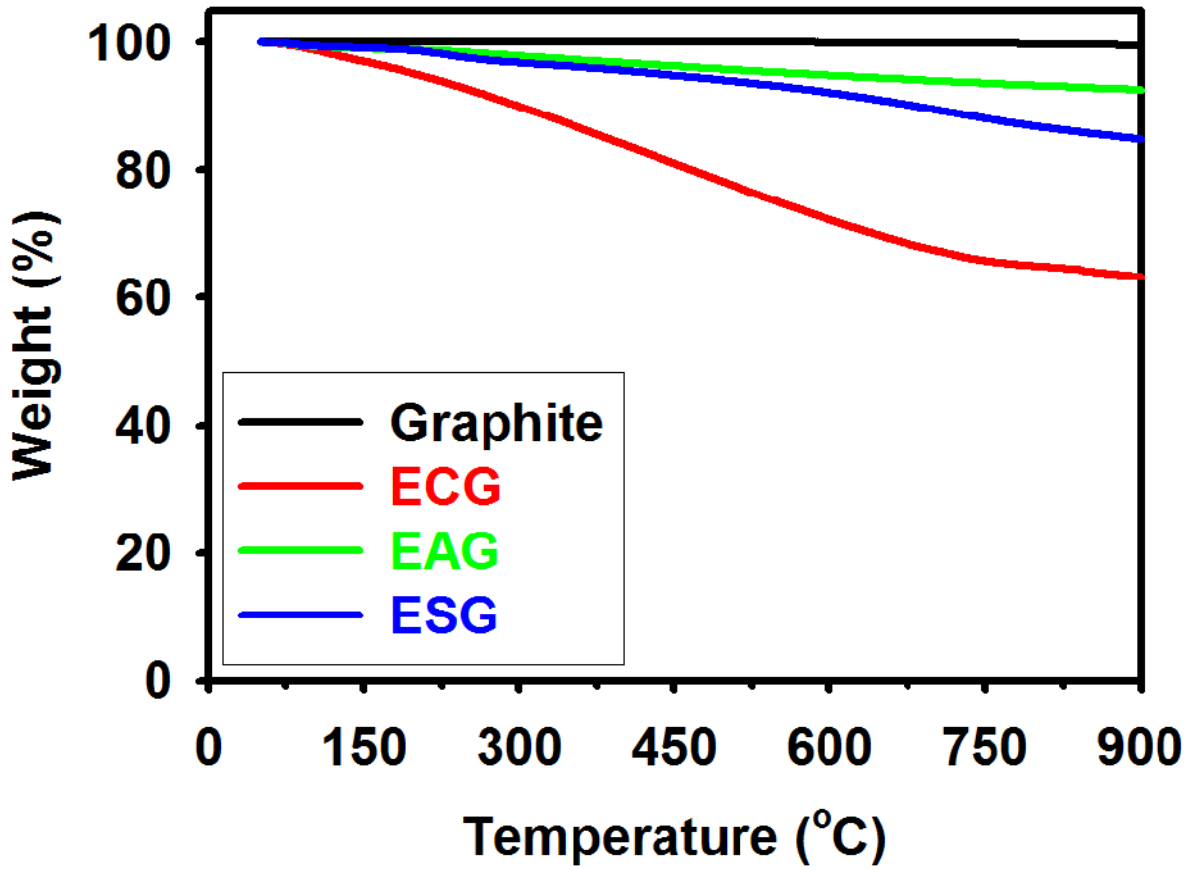

Fig. S16. TGA thermograms obtained from EAG and ESG samples prepared by ball milling for 48 hours in the presence of NH_3 and SO_3, respectively. The heating rate was 10 °C/min in nitrogen atmosphere. TGA thermograms from the pristine graphite and ECG are also included for comparison.

Supporting video legends

Video S1. Video clip showing sparkling while ball mill capsule is opening in air moisture.

Video S2. Video clip showing no sparkling while ball mill capsule is opening in dry room (moisture level is less than 100 ppm).

Video S3. Video clip showing no sparkling while ball mill capsule is opening in vinyl bag containing nitrogen/moisture (80/20, v/v).

Table S1. Elemental analysis of the ECG samples collected at different ball-milling times.

Milling Time (h)	C (%)	H (%)	N (%)	O (%)	C/N	C/O
0	99.64	BDL[a]	BDL	0.13	∞	1021
24	96.68	0.38	BDL	2.66	∞	48
36	90.83	0.78	BDL	5.54	∞	22
48	72.04	1.01	BDL	26.46	∞	4
60	71.88	1.03	BDL	26.44	∞	4
72	71.72	1.08	BDL	26.74	∞	4
Air-48h	83.68	0.36	3.02	7.01	32	16

a. BDL = Below detection limit.

Table S2. EA, XPS, EDX, and TGA data of the pristine graphite and ECG after the ball milling for 48 hours

Sample	Element	EA	XPS	TGA (Char yield in N_2)	
				at 800 °C (%)	at 1000 °C (%)
Graphite	C (%)	99.64	98.35	99.7	99.1
	H (%)	BDL[a]	NA[b]		
	O (%)	0.13	1.65		
	C/O	1021	79.4		
ECG	C (%)	72.04	82.22	64.9	61.8
	H (%)	1.01	NA[b]		
	O (%)	26.46	17.78		
	C/O	3.63	6.16		
GO	C (%)	48.92	32.53	48.1	44.6 (900 °C)
	H (%)	2.13	NA[b]		
	O (%)	45.45	67.47		
	C/O	1.43	0.64		

a. BDL = Below detection limit or not available.

b. NA = Not applicable.

Table S3. BET surface areas, pore volumes and pore sizes of samples

Sample	Surface Area (m^2/g)	Pore Volume (mL/g)	Pore Size (Å)
Graphite	2.8	0.0016	22.667
ECG	389.4	0.1841	18.912
H-ECG	631.8	0.2904	18.385
GO	29.8	0.0147	19.668
H-GO	92.1	0.0463	20.140

Table S4. Electrical properties of graphite, ECG, HECG, GO and H-GO. In case of H-GO, indicated by (*), samples were shattered by direct annealing of GO to produce H-GO at 900 °C.

Sample	Form	Conductivity (S/cm)
ECG	Pellet	1.1×10^{-2}
H-ECG	Pellet	38
GO	Pellet	1.6×10^{-5}
H-GO*	NA	NA
H-ECG	Free-standing film	1214
H-GO*	NA	NA

Table S5. Elemental analysis of EAG and ESG

Sample	C (%)	H (%)	N (%)	O (%)	S (%)
Graphite	99.64	BDL[a]	NA[b]	0.13	NA[b]
ECG	72.04	1.01	NA[b]	26.46	NA[b]
EAG	88.83	1.21	4.49	3.69	NA[b]
ESG	79.58	0.62	NA[b]	9.36	9.35

a. BDL = Below detection limit.

b. NA = Not applicable.

Note: Pristine graphite and ECG after 48 h ball milling are presented for comparison

Table S6. Comparison of general characteristics of ECG and GO

	ECG	GO	Advantages for ECG	Ref.
History	2011: Invention	1860: Brodie (S13) 1898: Staudenmaier (S14) 1958: Hummers (S15)	GO has known for longer than 150 years	S13 S14 S15
Reactant	Graphite + CO_2	Graphite + $NaNO_3$, $KMnO_4$, H_2SO_4 (S15)	ECG is eco-friendly process	S15
Yield	Very high (~quantitative)	Low	Only limited by the size of the ball milling chamber	
Interlayer d-spacing (Å)	Broad	6.67 ~7.70 (S15)	Graphite=3.4	S15
C/O ratio (EA)	3.63	2.25 (S15)	timeless C-basal plane damage	S15
BET surface area (m^2/g)	389.4	29.8	139 times higher	
I_D/I_G ratio	1.15	1.03 (S16)	Depending on reaction time	S16
Functional Groups	Carboxylic acid only	Various (Carboxylic Acid, Carbonyl, Aldehyde, Epoxy, Hydroxyl etc.) (S17)	Well-defined functional groups could be further selectively modified by using carboxylic acid reaction	S17
Functional Groups Selectivity	Selective	Non-selective	Highly selective, but other functional groups can also be selectively introduced via the ball milling process (*e.g.*, amine and sulfonic acid)	
Regio-selectivity	Edge only	Edge + Basal plane (S18)	Region-specific	S18
Powder Conductivity (S/cm)	1.1×10^{-2}	6×10^{-7} (S18) 6.8×10^{-10} (S19)	Much higher conductivity (Graphite = 10~1400) (S20)	S18 S19 S20
Char yield at 800 °C in N_2	< 65%	< 60% (S21)	ECG has better thermal stability	S21
Diapersibility in basic solvents	Good	Good	Higher stable concentration (~three times in NMP)	
Zeta-potential (mV)	-34.2 (NMP) -41.6 (Water, pH=10)	-35.1 (NMP) -43.0 (Water, pH=10) (S22)	Similar	S22

References

S1. Bae S, *et al*. (2010) Roll-to-roll production of 30-inch graphene films for transparent electrodes. *Nat Nanotechnol* 5: 574-578.

S2. Lerf A, He H, Forster M & Klinowski J (1998) Structure of graphite oxide revisited. *J Phys Chem B* 102: 4477-4482.

S3. Gao W, Alemany LB, Ci L, & Ajayan PM (2009) New insights into the structure and reduction of graphite oxide. *Nat Chem* 1: 403-408.

S4. Stankovich S, Piner RD, Nguyen ST & Ruoff RS (2006) Synthesis and exfoliation of isocyanate-treated graphene oxide nanoplatelets. *Carbon* 44: 3342-3347.

S5. Collins PG, Bradley K, Ishigami M, & Zettl A (2000) Extreme oxygen sensitivity of electronic properties of carbon nanotubes. *Science* 287: 1801-1804.

S6. Pei S, *et al*. (2010) Direct reduction of graphene oxide films into highly conductive and flexible graphene films by hydrohalic acids. *Carbon* 48: 4466-4474.

S7. Watcharotone S, *et al.* (2007) Graphene−silica composite thin films as transparent conductors. *Nano Lett* 7: 1888-1892.

S8. Akhavan O (2010) The effect of heat treatment on formation of graphene thin films from graphene oxide nanosheets. *Carbon* 48: 509-519.

S9. Wang Y, *et al.* (2010) Nitrogen-doped graphene and its application in electrochemical biosensing. *ACS Nano* 4: 1790-1798.

S10. Wang H, *et al.* (2010) Effect of graphene oxide on the properties of its composite with polyaniline. *ACS Appl Mater Interfaces* 2: 821-828.

S11. Wang S, Yu D & Dai L (2011) Polyelectrolyte functionalized carbon nanotubes as efficient metal-free electrocatalysts for oxygen reduction. *J Am Chem Soc* 133: 5182-5185.

S12. Fenske MR, *et al.* (1947) Raman spectra of hydrocarbons. *Anal. Chem.* 19: 700-765.

S13. Brodie BC (1860) Sur le poids atomique du graphite [On the atomic weight of graphite]. *Ann Chim Phys* 59: 466-472. French

S14. Staudenmaier L (1898) Verfahren zur darstellung der graphitsäure [Procedures for the presentation of the graphite-acid]. *Ber Dtsch Chem Ges* 31: 1481-1487. German

S15. Hummers WS & Offeman RE (1958) Preparation of graphitic oxide. *J Am Chem Soc* 80: 1339.

S16. Huang L, *et al.* (2011) Pulsed laser assisted reduction of graphene oxide. *Carbon* 49: 2431-2436.

S17. Dreyer DR, Park S, Bielawski CW & Ruoff RS (2010) The chemistry of graphene oxide. *Chem Soc Rev* 39: 228-240.

S18. Xu Y, *ea al.* (2008) Flexible graphene films via the filtration of water-soluble noncovalent functionalized graphene sheets. *J Am Chem Soc* 130: 5856-5857.

S19. Shin H-J, *et al.* (2009) Efficient reduction of graphite oxide by sodium borohydride and its effect on electrical conductance. *Adv Funct Mater* 19: 1987-1992.

S20. Deprez N & McLachlan DS (1988) The analysis of the electrical conductivity of graphite conductivity of graphite powders during compaction. *J Phys D: Appl Phys* 21: 101-107.

S21. Goncalves G, *et al.* (2010) Graphene oxide modified with PMMA via ATRP as a reinforcement filler. *J Mater Chem* 20: 9927-9934.

S22. Li D, et al. Processable aqueous dispersions of graphene nanosheets. *Nat Nanotechol* 3: 101-105.